J|A|C|S
ARTICLES
Published on Web 02/20/2002

Six-Coordinate and Five-Coordinate $Fe^{II}(CN)_2(CO)_x$ Thiolate Complexes ($x = 1, 2$): Synthetic Advances for Iron Sites of [NiFe] Hydrogenases

Wen-Feng Liaw,*,† Jiun-Hung Lee,† Hung-Bin Gau,† Chien-Hong Chen,† Shiou-Ju Jung,† Chen-Hsiung Hung,† Wen-Yuan Chen,† Ching-Han Hu,† and Gene-Hsiang Lee‡

Contribution from the Department of Chemistry, National Changhua University of Education, Changhua 50058, Taiwan, and Instrumentation Center, National Taiwan University, Taipei 10764, Taiwan

Received June 20, 2001

Abstract: The dicyanodicarbonyliron(II) thiolate complexes *trans*,*cis*-$[(CN)_2(CO)_2Fe(S,S-C-R)]^-$ (R = OEt (**2**), $N(Et)_2$ (**3**)) were prepared by the reaction of [Na][S−C(S)−R] and $[Fe(CN)_2(CO)_3(Br)]^-$ (**1**). Complex **1** was obtained from oxidative addition of cyanogen bromide to $[Fe(CN)(CO)_4]^-$. In a similar fashion, reaction of complex **1** with [Na][S,O−C_5H_4N], and [Na][S,N−C_5H_4] produced the six-coordinate *trans*,*cis*-$[(CN)_2(CO)_2Fe(S,O-C_5H_4N)]^-$ (**6**) and *trans*,*cis*-$[(CN)_2(CO)_2Fe(S,N-C_5H_4)]^-$ (**7**) individually. Photolysis of tetrahydrofuran (THF) solution of complexes **2**, **3**, and **7** under CO led to formation of the coordinatively unsaturated iron(II) dicyanocarbonyl thiolate compounds $[(CN)_2(CO)Fe(S,S-C-R)]^-$ (R = OEt (**4**), $N(Et)_2$ (**5**)) and $[(CN)_2(CO)Fe(S,N-C_5H_4)]^-$ (**8**), respectively. The IR ν_{CN} stretching frequencies and patterns of complexes **4**, **5**, and **8** have unambiguously identified two CN^- ligands occupying cis positions. In addition, density functional theory calculations suggest that the architecture of five-coordinate complexes **4**, **5**, and **8** with a vacant site trans to the CO ligand and two CN^- ligands occupying cis positions serves as a conformational preference. Complexes **2**, **3**, and **7** were reobtained when the THF solution of complexes **4**, **5**, and **8** were exposed to CO atmosphere at 25 °C individually. Obviously, CO ligand can be reversibly bound to the Fe^{II} site in these model compounds. Isotopic shift experiments demonstrated the lability of carbonyl ligands of complexes **2**, **3**, **4**, **5**, **7**, and **8**. Complexes $[(CN)_2(CO)Fe(S,S-C-R)]^-$ and NiA/NiC states [NiFe] hydrogenases from *D. gigas* exhibit a similar one-band pattern in the ν_{CO} region and two-band pattern in the ν_{CN} region individually, but in different positions, which may be accounted for by the distinct electronic effects betwen $[S,S-C-R]^-$ and cysteine ligands. Also, the facile formations of five-coordinate complexes **4**, **5**, and **8** imply that the strong σ-donor, weak π-acceptor CN^- ligands play a key role in creating/stabilizing five-coordinate iron(II) $[(CN)_2(CO)Fe(S,S-C-R)]^-$ complexes with a vacant coordination site trans to the CO ligand.

Introduction

An intriguing common feature in the active sites of [Fe]-only and [NiFe] hydrogenase metalloproteins is the presence of at least one Fe center coordinated by CO and CN^- ligands and a vacant coordination site at iron that may bind small molecules (e.g., H_2, H^+, H^-).[1−8] The active site of [NiFe] hydrogenase isolated from *Desulfovibrio gigas* consists of a $(S_{cys})_2Ni(\mu\text{-}S_{cys})_2(\mu\text{-}X)Fe(CO)(CN)_2$ (X = O, OH) bimetallic complex that can exist in various redox states.[1] The iron site in the active form has been established as a pyramidal $[Fe(CN)_2(CO)]$ unit with the opposite face coordinated to two cysteines bridged to a nickel (a pyramidal [Fe(CN)(CO)(SO)] unit was

† National Changhua University of Education.
‡ National Taiwan University.

(1) (a) Volbeda, A.; Charon, M.-H.; Piras, C.; Hatchikian, E. C.; Frey, M.; Fontecilla-Camps, J. C. *Nature* **1995**, *373*, 580. (b) Volbeda, A.; Garcin, E.; Piras, C.; de Lacey, A. L.; Fernandez, V. M.; Hatchikian, E. C.; Frey, M.; Fontecilla-Camps, J. C. *J. Am. Chem. Soc.* **1996**, *118*, 12989. (c) Garcin, E.; Vernede, X.; Hatchikian, E. C.; Volbeda, A.; Frey, M.; Fontecilla-Camps, J. C. *Structure* **1999**, *7*, 557. (d) Happe, R. P.; Roseboom, W.; Pierik, A. J.; Albracht, S. P.; Bagley, K. A. *Nature* **1997**, *385*, 126. (e) Frey, M. *Struct. Bonding* **1998**, *90*, 98.

(2) (a) Nicolet, Y.; Piras, C.; Legrand, P.; Hatchikian, E. C.; Fontecilla-Camps, J. C. *Structure* **1999**, *7*, 13. (b) Nicolet, Y.; De Lacey, A. L.; Vernede, X.; Fernandez, V. M.; Hatchikian, E. C.; Fontecilla-Camps, J. C. *J. Am. Chem. Soc.* **2001**, *123*, 1596. (c) Peters, J. W.; Lanzilotta, W. N.; Lemon, B. J.; Seefeldt, L. C. *Science* **1998**, *282*, 1853. (d) De Lacey, A. L.; Stadler, C.; Cavazza, C.; Hatchikian, E. C.; Fernandez, V. M. *J. Am. Chem. Soc.* **2000**, *122*, 11232. (e) Popescu, C. V.; Münck, E. *J. Am. Chem. Soc.* **1999**, *121*, 7877.

(3) (a) Higuchi, Y.; Ogata, H.; Miki, K.; Yasuoka, N.; Yagi, T. *Structure* **1999**, *7*, 549. (b) Higuchi, Y.; Yagi, T.; Yasuoka, N. *Structure* **1997**, *5*, 1671.

(4) (a) de Lacey, A. L.; Hatchikian, E. C.; Volbeda, A.; Frey, M.; Fontecilla-Camps, J. C.; Fernandez, V. M. *J. Am. Chem. Soc.* **1997**, *119*, 7181. (b) Davidson, G.; Choudhury, S. B.; Gu, Z.; Bose, K.; Roseboom, W.; Albracht, S. P. J.; Maroney, M. J. *Biochemistry* **2000**, *39*, 7468. (c) Hatchikian, E. C.; Traore, A. S.; Fernandez, V. M.; Cammack, R. *Eur. J. Biochem.* **1990**, *187*, 635. (d) Happe, R. P.; Roseboom, W.; Albracht, S. P. J. *Eur. J. Biochem.* **1999**, *259*, 602. (e) Van der Zwaan, J. W.; Coremans, J. M. C. C.; Bouwens, E. C. M.; Albracht, S. P. J. *Biochim. Biophys. Acta* **1990**, *1041*, 101. (f) Liaw, W.-F.; Chen, C.-H.; Lee, C.-M.; Lee, G.-H.; Peng, S.-M. *J. Chem. Soc., Dalton Trans.* **2001**, 138.

(5) (a) Lemon, B. J.; Peters, J. W. *J. Am. Chem. Soc.* **2000**, *122*, 3793. (b) Lemon, B. J.; Peters, J. W. *Biochemistry* **1999**, *38*, 12969. (c) Bennett, B.; Lemon, B. J.; Peters, J. W. *Biochemistry* **2000**, *39*, 7455.

10.1021/ja011504f CCC: $22.00

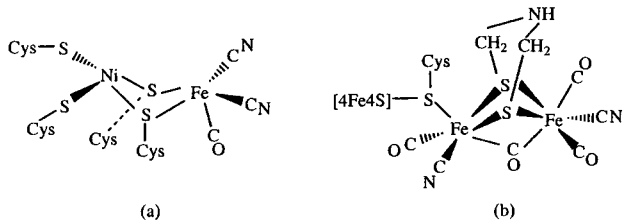

Figure 1. (a) Schematic drawing of the active site of [NiFe] hydrogenases as deduced from crystallographic studies.[1] (b) Schematic drawing of the H-cluster of the CO-inhibited form of *Clostridium pasteuranium* [Fe] hydrogenases as deduced from recent X-ray crystallographic studies.[2,5]

proposed in [NiFe] hydrogenases isolated from *D. vulgaris Miyazaki F.*[2]).[1] Thus, a vacant coordination site around iron, trans to the carbonyl ligand, appears to be a reactive site and presumably plays an important role in biological hydrogen activation.[1,3,4,6] The nickel site has been proposed to be redox active, while the iron site remains as Fe(II) in all spectroscopically defined redox states of the enzyme.[4] Also, direct evidence has shown that redox states C/SI can bind external CO in [NiFe] hydrogenases.[4] The exogenously added CO molecule is known to inhibit activity in [NiFe] hydrogenases, and is bound to metal in the active site in an end-on way, although it is not clear yet to which metal, Ni or Fe (nickel was proposed as the binding site of CO molecule recently).[4] A schematic drawing of the active site of [NiFe] hydrogenases as deduced from crystallographic studies is shown in Figure 1a.[1]

The recent report of high-quality X-ray crystal structure of [Fe]-only hydrogenases from *Desulfovibrio desulfuricans* revealed that the active site contains a dinuclear iron di(thiomethyl)amine with mixed CO and CN^- ligands bound to a [4Fe−4S] cluster via cysteine bridge, and also suggested that the unsaturated Fe center present in the H-cluster of the enzyme acts as a H_2 binding site.[2] The extrinsic CO binds to the distal Fe atom of the H-cluster, and is vibrationally coupled to the intrinsic CO ligand at this Fe atom.[2d] Upon reduction of the active oxidized form, FTIR spectroscopic evidence and crystal structure of the reduced active site of *D. desulfuricans* [Fe] hydrogenase show that the previously bridging CO is now terminally bound to the distal iron that most likely serves as the primary hydrogen binding site.[2b] A schematic drawing of the H-cluster of the CO-inhibited form of the *Clostridium pasteuranium* [Fe] hydrogenases as deduced from recent X-ray crystallographic studies is shown in Figure 1b.[2d,5] Additionally, recent investigations indicate that carbon monoxide causes reversible inhibition of hydrogen oxidation, and that inhibition can be reversed by illuminating with light in *Clostridium pasteuranium* [Fe] hydrogenase.[5]

The roles of CN^- and CO ligands, the function of dithiolate bridge/protein-bound cysteine bridge, the active site construction, the photochemical properties of the CO-inhibited form, and the requirement of two metals in the active sites of [Fe] and [NiFe] hydrogenases (homodinuclear iron−iron in [Fe] hydrogenases and heterodinuclear nickel−iron in the case of [NiFe] hydrogenases) are the principal questions to be raised.[1−8] Designing and synthesizing structural model complexes, in addition to serving as spectroscopic references, may provide essential understanding about the active site construction and function of [Fe] and [NiFe] hydrogenases, and the roles/functions of CO and CN^- ligands, and may elucidate the electronic structure of active centers of the binuclear subcluster.[9−14] Two iron thiolate cyanocarbonyl model complexes have been reported recently by Darensbourg et al.,[9] Rauchfuss et al.,[11] Pickett et al.,[12] and Koch et al.[10] In one interesting model compound each iron of the dinuclear Fe(I) thiolate cyanocarbonyl complex is surrounded by one CN^- and two CO ligands,[9,11,12] while the other model compound is a low-spin six-coordinate, mononuclear iron(II)/iron(III) thiolate complex with mixed CO and CN^- ligands.[10] Recent work in this laboratory has shown that a dinuclear iron(II) thiolate cyanocarbonyl $[Fe(CO)_2(CN)(\mu\text{-}S,S{-}C_6H_4)]_2^{2-}$ complex was produced upon protonation of five-coordinate mononuclear iron(II) thiolate cyanocarbonyl complex $[Fe(CO)_2(CN)(S,NH{-}C_6H_4)]^-$ by 1,2-benzenedithiol.[13]

Examples of cyanide (CN^-) coordination to iron(II) and the spectroscopic signals of dicyanide iron(II) thiolate carbonyl complexes ($[(CN)_2(CO)Fe^{II}(SR)_2]^{n-}$) are of much interest, particularly in catalytically active site construction of the $(CysS)_2Ni(\mu\text{-}SCys)_2Fe(CN)_2(CO)$ active site of [NiFe] hydrogenases. As far as we know, there is no report of the dicyanide iron(II) thiolate carbonyl complexes characterized by X-ray crystallography.[15,16] By application of oxidative addition and stepwise ligand exchange route, we have prepared *trans,cis*-$[(CN)_2(CO)_2Fe(S,S{-}C{-}R)]^-$ (R = OEt (**2**), R = $N(Et)_2$ (**3**)), *trans,cis*-$[(CN)_2(CO)_2Fe(S,\ O{-}C_5H_4N)]^-$ (**6**), and *trans,cis*-$[(CN)_2(CO)_2Fe(S,N{-}C_5H_4)]^-$ (**7**). These along with the precursor complex $[(CN)_2(CO)_3Fe(Br)]^-$ (**1**) were isolated and characterized by X-ray crystallography and infrared spectroscopy.

Results and Discussion

When cyanogen bromide (0.8 mmol) was reacted directly with [PPN][$Fe(CO)_4(CN)$] (0.5 mmol)[17]in tetrahydrofuran (THF) at room temperature, air-stable hexacoordinate Fe^{II} complex [PPN]-$[(CN)_2(CO)_3Fe(Br)]$ (**1**) was isolated as a light yellow solid after recrystallization from THF−hexane (yield 75%) (Scheme 1a). An oxidative addition/decarbonylation reaction may account for the formation of complex **1**.[18]

Subsequent reactions of complex **1** with [Na][S−C(S)−R] (R = OEt, $N(Et)_2$) in THF/CH_2Cl_2 produced the air and

(6) (a) Darensbourg, M. Y.; Lyon, E. J.; Smee, J. J. *Coord. Chem. Rev.* **2000**, *206*, 533. (b) Adams, M. WW; Stiefel, E. I. *Curr. Opin. Chem. Biol.* **2000**, *4*, 214.
(7) *Bioinorganic Catalysis*, 2nd ed.; Cammack, R., van Vliet, P., Reedijk J., Eds.; Marcel Dekker: New York, 1999; p 231.
(8) Adams, M. W. W.; Stiefel, E. I. *Science* **1998**, *282*, 1842.
(9) Lyon, E. J.; Georgakaki, I. P.; Reibenspies, J. H.; Darensbourg, M. Y. *Angew. Chem., Int. Ed.* **1999**, *38*, 3178.
(10) Hsu, H.-F.; Koch, S. A.; Popescu, C. V.; Münck, E. *J. Am. Chem. Soc.* **1997**, *119*, 8371.
(11) Schmidt, M.; Contakes, S. M.; Rauchfuss, T. B. *J. Am. Chem. Soc.* **1999**, *121*, 9736.
(12) Le cloirec, A.; Best, S. P.; Borg, S.; Davies, S. C.; Evans, D. J.; Hughes, D. L.; Pickett, C. J. *J. Chem. Soc., Chem. Commun*. **1999**, 2285.
(13) Liaw, W.-F.; Lee, N.-H.; Chen, C.-H.; Lee, C.-M.; Lee, G.-H.; Peng, S.-M. *J. Am. Chem. Soc.* **2000**, *122*, 488.
(14) (a) Gu, Z.; Dong, J.; Allan, C. B.; Choudhury, S. B.; Franco, R.; Moura, J. J. G.; Moura, I.; LeGall, J.; Przybyla, A. E.; Roseboom, W.; Albracht, S. P. J.; Axley, M. J.; Scott, R. A.; Maroney, M. J. *J. Am. Chem. Soc.* **1996**, *118*, 11155. (b) Colpas, G. J.; Day, R. O.; Maroney, M. J. *Inorg. Chem.* **1992**, *31*, 5053. (c) Roberts, L. M.; Lindahl, P. A. *J. Am. Chem. Soc.* **1995**, *117*, 2565. (d) Marganian, C. A.; Vazir, H.; Baidya, N.; Olmstead, M. M.; Mascharak, P. K. *J. Am. Chem. Soc.* **1995**, *117*, 1584. (e) Davies, S. C.; Evans, D. J.; Hughes, D. L.; Longhurst, S.; Sanders, J. R. *J. Chem. Soc., Chem. Commun*. **1999**, 1935. (f) Sellmann, D.; Geipel, F.; Moll, M. *Angew. Chem., Int. Ed*. **2000**, *39*, 561.
(15) (a) Lai, C.-H.; Lee, W.-Z.; Miller, M. L.; Reibenspies, J. H.; Darensbourg, D. J.; Darensbourg, M. Y. *J. Am. Chem. Soc.* **1998**, *120*, 10103. (b) Darensbourg, D. J.; Reibenspies, J. H.; Lai, C.-H.; Lee, W.-Z.; Darensbourg, M. Y. *J. Am. Chem. Soc.* **1997**, *119*, 7903.
(16) Moreland, A. C.; Rauchfuss, T. B. *Inorg. Chem.* **2000**, *39*, 3029.
(17) (a) Ruff, J. K. *Inorg. Chem.* **1969**, *8*, 86. (b) Goldfield, S. A.; Raymond, K. N. *Inorg. Chem.* **1974**, *13*, 770.

Scheme 1

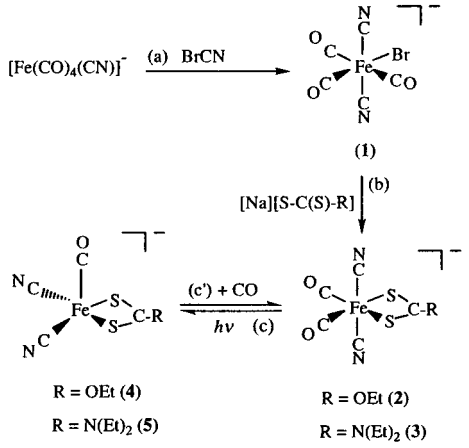

Table 1. Infrared Data for Complexes **1**−**8**

compound	ν(CN), cm^{-1} (THF)	ν(CO), cm^{-1} (THF)
1	2139 vw, 2127 vw	2099 m, 2056 s, 2035 m
2	2122 vw, 2112 w	2038 vs, 1984 vs
3	2119 vw, 2112 w	2027 vs, 1973 vs
4	2113 w, 2105 w	1996 vs
5	2109 w, 2102 w	1985 vs
6	2121 vw, 2109 w	2041 vs, 1982 vs
7	2124 vw, 2113 w	2036 vs, 1983 vs
8	2111 w, 2103 w	1996 vs

thermally stable, yellow *trans,cis*-[PPN][$(CN)_2(CO)_2$Fe(S,S−C−R)] complexes (R = OEt (**2**), $N(Et)_2$ (**3**)) individually (Scheme 1b).[4,6a] The IR spectrum of complex **2** in the aprotic solvent THF reveals two weak absorption bands for the CN^- ligands at 2122 vw and 2112 w cm^{-1} (2119 vw and 2112 w cm^{-1} for **3**) supporting a trans position of two CN^- ligands, while the two strong absorption bands 2038 s, 1984 s cm^{-1} (2027 s, 1973 s cm^{-1} for **3**) assigned to the carbonyl stretching frequencies support a cis position of two CO ligands (Table 1).[19] When a THF solution of complex **3** is purged with ^{13}CO, the IR ν_{CO} peaks at 2027, 1973 cm^{-1} shift to absorbances at 1981 s, 1928 s cm^{-1} (*trans,cis*-[$(CN)_2(^{13}CO)_2$Fe(S,S−C−$N(Et)_2$)]$^-$). The isotopic shift of 45 cm^{-1} is consistent with the calculated position, based only on the difference in masses between ^{12}CO and ^{13}CO. The reappearance of the 2027, 1973 cm^{-1} bands on removal of the ^{13}CO and replacement with ^{12}CO atmosphere demonstrated reversibility of CO ligand lability of complexes **3**.

In contrast, the isotopic shift of ν_{CO} was almost not observed when complex **2** was treated with 1 atm of ^{13}CO in THF at room temperature overnight. We noticed that the distinct electronic effects between diethyl dithiocarbamate ([S,S−CN-$(Et)_2$]$^-$) and ethyl xanthate ([S,S−COEt]$^-$) ligands has a significant effect on CO ligand lability of *trans,cis*-[$(CN)_2$-$(CO)_2$Fe(S,S−C−R)]$^-$ complexes.[20]

Upon photolysis of THF solution of complex **2** (or **3**) under CO atmosphere at room temperature, the IR ν_{CO} and ν_{CN} stretching frequencies and patterns 2038 s, 1984 s cm^{-1} (ν_{CO}) and 2122 vw, 2112 w cm^{-1} (ν_{CN}) (complex **3**: 2027 s, 1973 s cm^{-1} (ν_{CO}) and 2119 vw, 2112 w cm^{-1} (ν_{CN})) shifting to absorbances at 1996 s (ν_{CO}), 2113 w, 2105 w (ν_{CN}) cm^{-1} (1985 vs (ν_{CO}), 2109 w, 2102 w (ν_{CN}) cm^{-1}) is consistent with the formation of coordinatively unsaturated iron(II) dicyanide carbonyl thiolate complex [PPN][$(CN)_2$(CO)Fe(S,S−COEt)] (**4**) ([PPN][$(CN)_2$(CO)Fe(S,S−CN$(Et)_2$)] (**5**)) (Table 1) with two cyanide ligands occupying cis positions (Figure 2a,b) (Scheme 1c).[1,4a] The ^{13}C (CO) NMR spectra (δ (CD_3CN) 210.79 (s) ppm for **4** and 212.5 (s) ppm for **5**) of complexes **4** and **5** also support the presence of the low-spin five-coordinate d^6 Fe(II) complexes

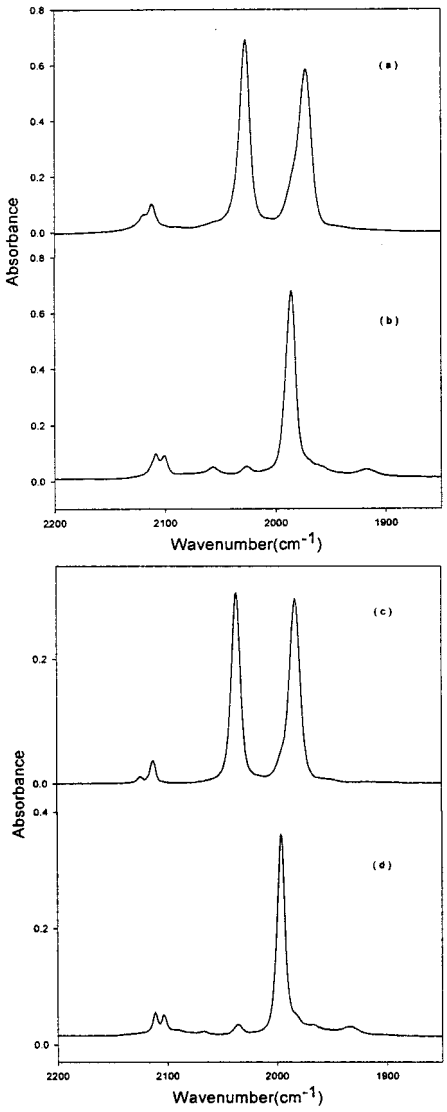

Figure 2. FTIR spectra (THF) of (a) complex **2**, (b) complex **4**, (c) complex **7**, and (d) complex **8**.

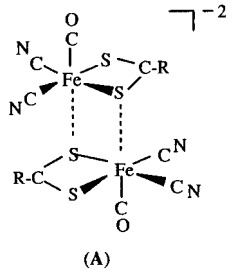

(A)

(18) (a) Liaw, W.-F.; Chiang, M.-H.; Liu, C.-J.; Harn, P.-J.; Liu, L.-K. *Inorg. Chem.* **1993**, *32*, 1536. (b) Liaw, W.-F.; Horng, Y.-C.; Ou, D.-S.; Ching, C.-Y.; Lee, G.-H.; Peng, S.-M. *J. Am. Chem. Soc.* **1997**, *119*, 9299. (c) Liaw, W.-F.; Hsieh, C.-K.; Lin, G.-Y.; Lee, G.-H. *Inorg. Chem.* **2001**, *40*, 3468.

(19) (a) Liaw, W.-F.; Chen, C.-H.; Lee, G.-H.; Peng, S.-M. *Organometallics* **1998**, *17*, 2370. (b) Liaw, W.-F.; Chen, C.-H.; Lee, C.-M.; Lin, G.-Y.; Ching, C.-Y.; Lee, G.-H.; Peng, S.-M. *J. Chem. Soc., Dalton Trans.* **1998**, 353.

(20) Cotton, F. A.; Wilkinson, G.; Murillo, C. A.; Bochmann, M. *Advanced Inorganic Chemistry*, 6th ed.; John Wiley and Sons: New York, 1999.

Table 2. Predicted Reaction Energy and Enthalpy for the Extrusion of CO from Complexes **2** and **3**[a,b]

	ΔE	ΔH(0 K)	ΔH(298 K)
2	0.0	0.0	0.0
4 + CO	32.3	29.6	30.5
4b + CO	35.0	32.4	33.2
4c + CO	42.6	39.8	40.7
4d + CO	45.4	42.6	43.5
3	0.0	0.0	0.0
5 + CO	30.5	27.9	28.7
5b + CO	33.7	31.3	32.1
5c + CO	44.4	41.7	42.6

[a] Refer to Figure 3 for species notation. [b] Values are in kcal/mol.

with two CN^- ligands occupying cis positions, respectively. However, we cannot unambiguously rule out the possibility of formation of the weak coordinative dimeric complex **A** in photolysis of THF solution of complexes **2** and **3**.

Density functional theory (DFT) was applied in this study. We used Becke's three-parameter hybrid functional,[21] where the exchange functional of Becke[22] and correlation functional of Lee, Yang, and Parr[23] were chosen (B3LYP). The geometries of all species studied were fully optimized using analytic gradients at the B3LYP/6-31G level. Harmonic vibrational frequency calculations were performed at the minima. The vibrational frequencies were used in the evaluation of zero-point vibrational energies and thermal corrections up to 298 K. Enthalpies were obtained at the B3LYP/6-31G*//B3LYP/6-31G level, including the thermal corrections obtained using B3LYP/6-31G. The GAUSSIAN 98 suite of programs has been used in this work.[24]

Relative energy (ΔE) and enthalpy (ΔH) computed of the species involved in the extrusion of CO from compounds **2** and **3** are summarized in Table 2. The structures and some of the important bond distances of these species are schematically illustrated in Figure 3. We have located four minima which correspond to the five-coordinate complex with the extrusion of the CO ligand from **2** (**4**, **4b**, **4c**, and **4d**; see Figure 3). Three minima were located corresponding to the extrusion of CO from **3** (**5**, **5b**, and **5c**; see Figure 3). A common feature is observed among these compounds: structures that are trigonal bypyramidal are more than 10 kcal/mol higher in energy than those that are square pyramidal (**4**, **4b** and **5**, **5b**). For the square pyramidal complexes, it was found that those having vacant sites trans to the CO ligand (**4** and **5**) are relatively stable. The observation is consistent with the proposal made by several research groups.[25−31]

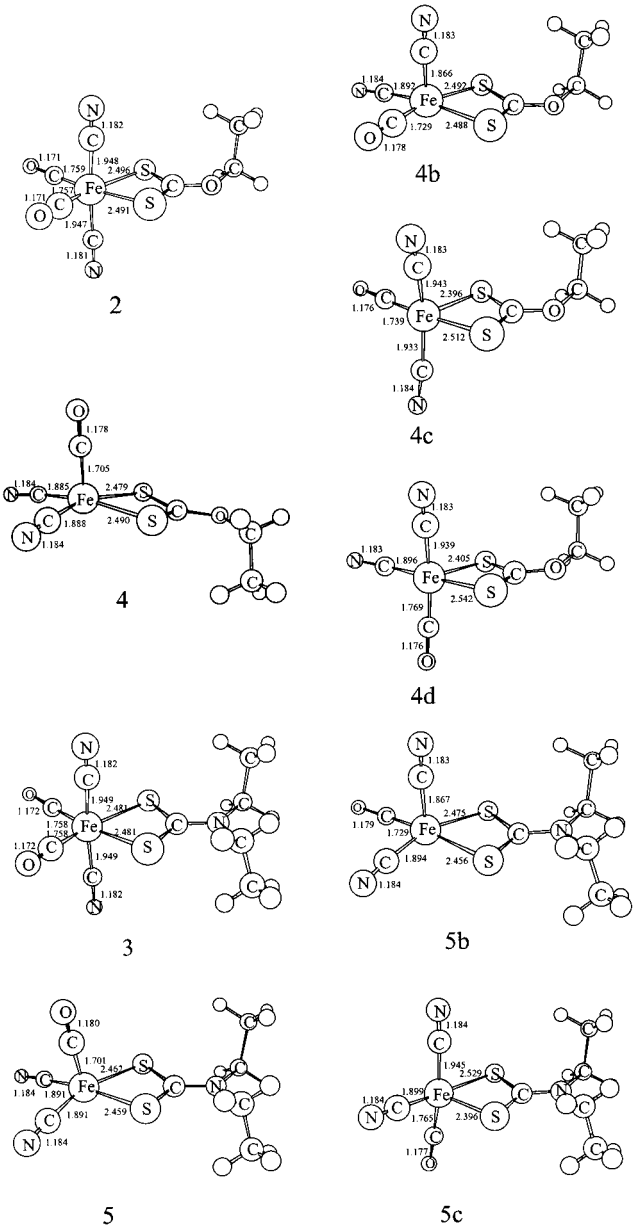

Figure 3. Structures and bond distances for the species involved in the extrusion of CO from **2** and **3**; geometries were optimized at the B3LYP/6-31G level.

The anionic complexes **4**, **5** and Ni-A/Ni-C states in [NiFe] hydrogenase from *D. gigas* exhibit a similar one-band pattern in the ν_{CO} region and two-band pattern in the ν_{CN} region individually,[4] but at different positions, 1996 vs (ν_{CO}), 2113 w, 2105 w (ν_{CN}) cm^{-1} (THF) for complex **4**, 1985 vs (ν_{CO}), 2109 w, 2102 w (ν_{CN}) for complex **5** (Table 1), and 1947 vs (ν_{CO}), 2093 w, 2083 w (ν_{CN}) cm^{-1} for Ni-A state [NiFe] hydrogenases

(21) Becke, A. D. *J. Chem. Phys.* **1993**, *98*, 5648.
(22) Becke, A. D. *J. Chem. Phys. Rev. A* **1988**, *A38*, 785.
(23) Lee, C.; Yang, W.; Parr, R. G. *Phys. Rev.* **1988**, *B37*, 785.
(24) Frisch, M. J.; Trucks, G. W.; Schlegel, H. B.; Scuseria, G. E.; Robb, M. A.; Cheeseman, J. R.; Zakrzewski, V. G.; Montgomery, Jr. J. A.; Stratmann, R. E.; Burant, J. C.; Dapprich, S.; Millam, J. M.; Daniels, A. D.; Kudin, K. N.; Strain, M. C.; Farkas, O.; Tomasi, J.; Barone, V.; Cossi, M.; Cammi, R.; Mennucci, B.; Pomelli, C.; Adamo, C.; Clifford, S.; Ochterski, J.; Petersson, G. A.; Ayala, P. Y.; Cui, Q.; Morokuma, K.; Malick, D. K.; Rabuck, A. d.; Raghavachari, K.; Foresman, J. B.; Cioslowski, J.; Ortiz, J. V.; Stefamov, B. B.; Martin, R. L.; Fox, D. J.; Keith, T.; Al-Laham, M. A.; Peng, C. Y.; Nanayakkara, A.; Gonzalez, C.; Challacombe, M.; Gill, P. M. W.; Johnson, B.; Chen, W.; Wong, M. W.; Andres, J. L.; Head-Gordon, M.; Replogle, E. S.; Pople, J. A. *GAUSSIAN 98*, Revision A.3, Gaussian, Inc.: Pittsburgh, PA, 1998.
(25) Chen, Y.; Petz, W.; Frenking, G. *Organometallics* **2000**, *19*, 2698.
(26) (a) Pierik, A. J.; Roseboom, W.; Happe, R. P.; Bagley, K. A.; Albracht, S. P. J. *J. Biol. Chem.* **1999**, *274*, 3331. (b) Van Der Spek, T. M.; Arendsen, A. F.; Happe, R. P.; Yun, S.; Bagley, K. A.; Stufkens, D. J.; Hagen, W. R.; Albracht, S. P. J. *Eur. J. Biochem.* **1996**, *237*, 629.
(27) (a) Garcin, E.; Vernede, X.; Hatchikian, E. C.; Volbeda, A.; Frey, M.; Fontecilla-Camps, J. C. *Struct. Folding Des.* **1999**, *7*, 557. (b) Higuchi, Y.; Ogata, H.; Miki, K.; Yasuoka, N.; Yagi, T. *Struct. Folding Des.* **1999**, *7*, 549.
(28) Wang, H.; Ralston, C. Y.; Patil, D. S.; Jones, R. M.; Gu, W.; Verhagen, M.; Adams, M.; Ge, P.; Riordan, C.; Maganian, C. A.; Maschrak, P.; Kovacs, J.; Miller, C. G.; Collins, T. J.; Brooker, S.; Croucher, P. D.; Wang, K.; Stiefel, E. I.; Cramer, S. P. *J. Am. Chem. Soc.* **2000**, *122*, 10544.
(29) Niu, S.; Thomson, L. M.; Hall, M. B. *J. Am. Chem. Soc.* **1999**, *121*, 4000.
(30) Dole, F.; Fournel, A.; Magro, V.; Hatchikian, E. C.; Bertrand, P.; Guigliarelli, B. *Biochemistry* **1997**, *36*, 7847.
(31) De Gioia, L.; Fantucci, P.; Guigliarelli, B.; Bertrand, P. *Inorg. Chem.* **1999**, *38*, 2658.

isolated from *D. gigas*,[4] which may be accounted for by the distinct electronic effects betwen $[S,S-C-R]^-$ (monoanionic ligand with S,S-donor atoms) and cysteine ligands.[15] This result is consistent with the conclusion, reported by Darensbourg et al., that the CO vibrational frequency to the electron density changes around Fe(II) center is about 2.6 times more sensitive than that for CN^-.[6a,15]

Exposure of complexes **4** and **5** to CO gives rise to changes in the IR spectra that are highly dependent on the temperature. Both **4** and **5** are unreactive toward CO at low temperature ($T < 0$ °C) in THF. Complex **3** was reobtained on exposure of the THF solution of complex **5** to CO atmosphere at 25 °C overnight. (Scheme 1c′). Presumably, here the structural rearrangements occur concurrently as CO ligand coordinated to the iron, and signify the low barriers of rearrangements of CO and CN^- ligands. The reversibility of CO ligand binding demonstrates that the complexes **3** and **5** are interconvertible. In contrast, complex **4** remains almost unchanged when treated with 1 atm of CO in THF at 25 °C overnight. Obviously, the two thiolates $[S,S-COEt]^-$ and $[S,S-C-N(Et)_2]^-$, rendering the $[(CN)_2(CO)Fe]$ unit in different electronic environments, induce differing stability to CO ligand. This observation may explain that nucleophiles, such as Et_3N and $[BH_4]^-$, do not react with the unsaturated $[(CN)_2(CO)Fe(S,S-C-R)]^-$ complexes with a vacant site trans to CO ligand in THF. The more effective electron-donating ligand $[S,S-C-N(Et)_2]^-$, compared with $[S,S-C-OEt]^-$, destabilizes the $[(CN)_2(CO)Fe^{II}]$ fragment (i.e., complex **5** is more apt to react with strong π-acceptor CO ligand). This is in contrast to the observation that the stronger π-donating bidentate $[S,NH-C_6H_4]^{2-}$ ligand stabilizes the unsaturated complex $[(CN)(CO)_2Fe(S,NH-C_6H_4)]^-$.[13] Coordinative association of the unsaturated complex $[(CN)(CO)_2Fe(S,S-C_6H_4)]^-$ leading to dinuclear $[(CN)(CO)_2Fe(S,S-C_6H_4)]_2^{2-}$ explains the instability of $[(CN)(CO)_2Fe(S,S-C_6H_4)]^-$ (π-donating ability, $[S,NH-C_6H_4]^{2-} > [S,S-C_6H_4]^{2-}$).[13,18c] These results imply that CN^- ligands play a key role in creating/stabilizing a five-coordinate Fe(II) $[(CN)_2(CO)Fe(S,S-C-R)]^-$ complex with a vacant coordination site trans to the CO ligand.[25]

With the aid of isotopic ^{13}CO labeling experiments, ν_{CO} and ν_{CN} vibrational spectroscopic studies also have unambiguously identified two CN^- ligands occupying cis positions in complexes **4** and **5**. Exposure of complex **4** to ^{13}CO gives rise to a one-band pattern (1953 cm^{-1}) of IR ν_{CO} bands at 25 °C for 3 days to afford ^{13}C-enriched derivative $[(CN)_2(^{13}CO)Fe(S,S-COEt)]^-$ (major) and a one-band pattern (1967 cm^{-1}) of IR ν_{CO} bands consistent with the observation that a single added CO molecule binds to the trans position of CO ligand to yield, presumably, the intermediate *cis,trans*-$[(CN)_2(^{13}CO)_2Fe(S,S-COEt)]^-$ (minor). Following extended periods of stirring at 25 °C for 10 days, a THF solution of complex **4** completely converted into *trans,cis*-$[(CN)_2(^{13}CO)_2Fe(S,S-COEt)]^-$ identified by its IR ν_{CO} bands at 1990 s, 1939 s cm^{-1} (THF). Here the "slow" rearrangement of *cis,trans*-$[(CN)_2(^{13}CO)_2Fe(S,S-C-OEt)]^-$ to the more stable *trans,cis*-$[(CN)_2(^{13}CO)_2Fe(S,S-C-OEt)]^-$ was adopted to explain the formation of $[(CN)_2(^{13}CO)Fe(S,S-C-OEt)]^-$ (major product) and *cis,trans*-$[(CN)_2(^{13}CO)_2Fe(S,S-C-OEt)]^-$ (minor product) in the initial reaction. Indeed, THF solution of complex **5** on stirring overnight also undergoes a ligand coordination/exchange process with ^{13}C-labeled carbon monoxide to afford *cis,trans*-$[(CN)_2(^{13}CO)_2Fe(S,S-C-N(Et)_2)]^-$

Scheme 2

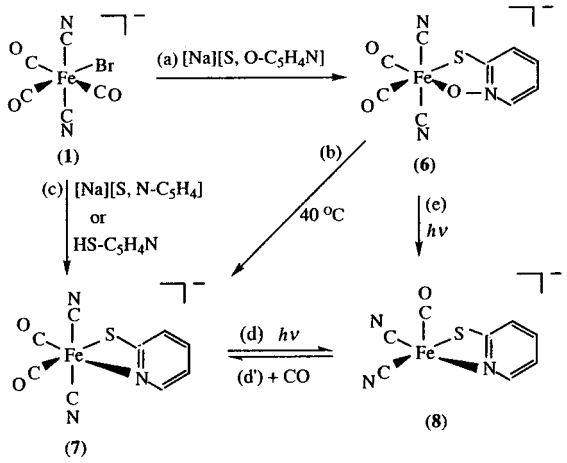

(ν_{CO} 1958 s cm^{-1}) (minor product) and ^{13}C-enriched derivative $[(CN)_2(^{13}CO)Fe(S,S-C-N(Et)_2)]^-$ (ν_{CO} 1944 cm^{-1}) (major product) at 25 °C. Following extended periods of stirring at room temperature for 5 days, complex **5** was completely transformed into *trans,cis*-$[(CN)_2(^{13}CO)_2Fe(S,S-C-N(Et)_2)]^-$. Studies of these model compounds imply that electronic effects transmitted to the $[(CN)_2(CO)Fe(S,S-C-R)]^-$ unit should be responsible for the optimized structure of the $[(CN)_2(CO)Fe(S,S-C-R)]^-$ and signify ease of substrate binding and release.

In a similar fashion, the ligand-displacement reaction was also displayed by complex **1** and $[Na][S,O-C_5H_4N]$. When a THF solution of complex **1** was treated with 1 equiv of $[Na][S,O-C_5H_4N]$, an immediate change in color from light yellow to dark brown was observed. The IR spectrum and X-ray crystal structure identified formation of the d^6 Fe(II) complex *trans,cis*-$[PPN][(CN)_2(CO)_2Fe(S,O-C_5H_4N)]$ (**6**) with a five-membered ring (bidentate, S,O-bonded) (Scheme 2a). The four-membered ring complex *trans,cis*-$[PPN][(CN)_2(CO)_2Fe(S,N-C_5H_4)]$ (**7**) (bidentate, S,N-bonded) was obtained via thermolytic conversion of complex **6** on heating (40 °C) in THF (Scheme 2b). This transformation slowly occurred at ambient temperature (25 °C), during which period no intermediate was detected spectrally. The loss of O atom from the Fe(II) center of complex **6** indicated the lability of O atom coordinated to $[Fe^{II}(CN)_2(CO)_2]$ unit and suggested that the bidentate $[S,N-C_5H_4]^-$ enhances the stability of $[Fe^{II}(CN)_2(CO)_2]$ unit. Complex **6** is the first example of an iron(II) cyanocarbonyl compound coordinated by mixed S and O atoms serving as a promising structural and functional model compound of the iron active site of [NiFe] hydrogenases, since most of the oxygen-tolerant hydrogenases allow the binding of the inhibitor (CO, sulfide, and O_2) in such a way that it can later be displaced.[1−8]

The S,N-bonded complex **7** was alternatively obtained via ligand-substitution reaction, a straightforward synthetic reaction of complex **1** with 1 equiv of $[Na][S,N-C_5H_4]$ (or $HS-C_5H_4N$) in THF (Scheme 2c). When THF solution of complex **7** was exposed to ^{13}CO overnight, absorbances at 1990 s, 1939 s cm^{-1} (*trans,cis*-$[(CN)_2(^{13}CO)_2Fe(S,N-C_5H_4)]^-$) appeared. Reappearance of the 2036 s, 1983 s cm^{-1} bands on removal of the ^{13}CO and replacement with ^{12}CO atmosphere demonstrated reversibility of CO ligand lability of complex **7**.

Theoretical computations provide some insights in the extrusion of CO from **7** (forming **8**); the structures are illustrated in Figure 4. In contrast to that of complexes **4** and **5**, only one

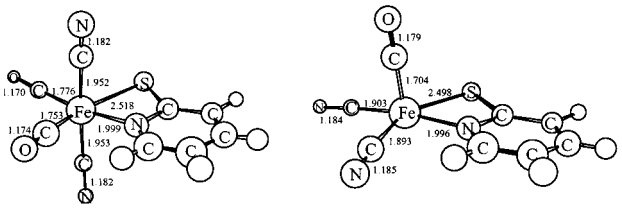

7 8

Figure 4. Structures and bond distances for the species involved in the extrusion of CO from **7**; geometries were optimized at the B3LYP/6-31G level.

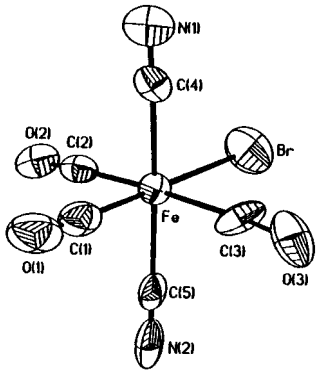

Figure 5. ORTEP drawing and labeling scheme of the $[(CN)_2(CO)_3Fe(Br)]^-$ anion with thermal ellipsoid drawn at 50% probability.

minimum was located. Complex **8** is square pyramidal with the vacant site trans to the CO ligand. At the B3LYP/6-31G*//B3LYP/6-31G level, the enthalpy of reaction is 26.0 kcal/mol.

To further add credibility to the CO ligand reversibly bound to the Fe^{II} site in these model compounds, a straightforward photolysis of THF solution of complex **7** under CO was also conducted at room temperature. The bands at 2125 vw, 2112 w (ν_{CN}) and 2036 s, 1983 s cm^{-1} (ν_{CO}) disappeared, with concomitant formation of a spectrum (2111 w, 2103 w (ν_{CN}) and 1996 cm^{-1} (ν_{CO}) (THF)) similar to that observed for complexes **4** and **5** (Figure 2c,d; Table 1), i.e., formation of five-coordinate $[(CN)_2(CO)Fe(S,N-C_5H_4)]^-$ (**8**) complex with two cyanide ligands occupying cis positions (Scheme 2d). Additionally, complex **7** displayed two distinct doublet signals (δ 214.4 (d), 210.0 (d) ppm (CD_3CN) ($J^{13}_{C,}{}^{13}_{C}$ = 9 Hz)) in the ^{13}C (CO) NMR spectra, consistent with the presence of two nonequivalent CO groups in the ^{13}C NMR spectra of complex **7** in acetonitrile-d_3 solution. The occurrence of one sharp singlet (δ 212.7 (s) ppm (CD_3CN)) ^{13}C (CO) NMR resonance was assigned to the CO group of complex **8**. The carbon monoxide atmosphere does promote the formation of complex **7** when complex **8** is exposed to 1 atm of CO in THF at room temperature for 2 days (Scheme 2d′).

Structure of Complex 1. The molecular structure of the complex **1** anion, Figure 5, is that of a distorted octahedron with C(5)−Fe−C(4) bond angle of 177.5(3)°. The Fe−C(N) average distance of 1.947(8) Å is significantly longer than those of the five-coordinate $[Fe(CO)_2(CN)(S,NH-C_6H_4)]^-$ (Fe−C(N) = 1.926(6) Å) and octahedral $[Fe(CO)(CN)(S,N-C_4H_3N)_2]^-$ (Fe−C(N) = 1.845(4) Å).[13] Further appropriate comparison lies in the C−N parameters: the C−N bond distance (average 1.015(8) Å) in complex **1** is significantly shorter than those of $[Fe(CO)_2(CN)(S,NH-C_6H_4)]^-$ (C−N = 1.137(6) Å) and $[Fe(CO)(CN)(S,N-C_4H_3N)_2]^-$ (C−N = 1.135(4) Å) (Table 3).[13]

Table 3. Selected Bond Distances (Å) and Angles (deg) for Complexes **1** and **2**

	Complex **1**		
Fe−C(4)	1.936(7)	Fe−C(5)	1.957(8)
C(4)−N(1)	1.017(8)	C(5)−N(2)	1.013(8)
Fe−C(1)	1.847(9)	Fe−C(2)	1.837(7)
Fe−C(3)	1.852(7)	C(1)−O(1)	1.029(9)
C(2)−O(2)	1.074(8)	C(3)−O(3)	1.037(8)
Fe−Br	2.459(1)		
C(2)−Fe−C(1)	90.0(3)	C(2)−Fe−C(3)	173.4(3)
C(2)−Fe−C(4)	94.0(3)	C(1)−Fe−C(4)	87.9(3)
C(2)−Fe−Br	91.4(2)	C(4)−Fe−C(5)	177.5(3)
	Complex **2**		
Fe−C(2)	1.778(11)	Fe−C(3)	1.810(10)
Fe−C(1)	1.919(10)	Fe−C(4)	1.955(10)
Fe−S(1)	2.300(3)	Fe−S(2)	2.326(3)
C(1)−N(1)	1.051(9)	C(4)−N(2)	1.137(11)
C(3)−O(1)	1.200(10)	C(2)−O(2)	1.149(10)
C(5)−O(3)	1.361(13)	C(6)−O(3)	1.464(14)
S(1)−Fe−S(2)	75.22(11)	C(2)−Fe−S(1)	171.3(3)
C(3)−Fe−S(1)	92.6(4)	C(1)−Fe−S(1)	91.2(3)
C(4)−Fe−S(1)	86.7(3)	N(1)−C(1)−Fe	178.4(11)
N(2)−C(4)−Fe	167.0(11)	C(1)−Fe−C(4)	177.4(4)

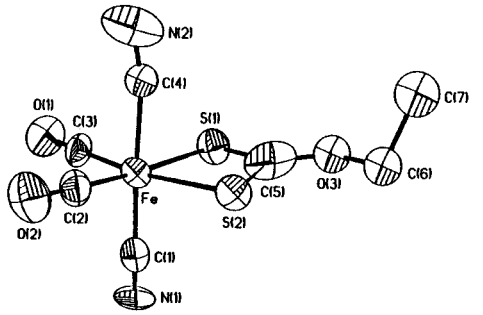

Figure 6. ORTEP drawing and labeling scheme of $[(CN)_2(CO)_2Fe(S,S-C-OEt)]^-$ with thermal ellipsoid drawn at 50% probability.

Structures of Complexes 2 and 3. Crystals of complexes **2** and **3** were found to have monoclinic $P2_1/c$ and $P2_1/n$ space group, respectively. Figure 6 displays a thermal ellipsoid plot of the anionic complex **2**. Selected bond distances and bond angles are given in Table 3. The constraints of the ethylxanthate ligand generates a S(1)−Fe−S(2) bond angle of 75.22(11)° enforcing a severe distortion from an octahedron at the six-coordinate iron site. The Fe−S(1) and Fe−S(2) bond lengths of 2.300(3) and 2.326(3) Å (unsymmetrical chelate), respectively, are within the range (2.2 Å) observed for [NiFe] hydrogenases from *D. gigas*.[1] The significantly shorter O(3)−C(5) bond (1.361(13) Å), as compared to 1.464(14) Å for the O(3)−C(6) bond, was attributed to the partial π-bond character between O(3) and C(5) atoms.[20]

The structure of the *trans,cis*-$[(CN)_2(CO)_2Fe(S,S-CN(Et)_2)]^-$ unit as $[PPN]^+$ salt is shown in Figure 7. The geometry about iron is a distorted octahedral, with the bite angle of the chelating $[S,S-CN(Et)_2]^-$ ligand being 75.02(6)° (Table 4). The Fe−S bonds of average length 2.316(2) Å (Fe(1)−S(1), 2.305(2) Å and Fe(1)−S(2), 2.327(2) Å), Fe−C(O) bonds of average length 1.798(6) Å, and Fe−C(N) bonds of average length 1.906(6) Å in complex **3** are within the range (2.2, 1.7, and 1.9 Å, respectively) observed in [NiFe] hydrogenases from *D. gigas*.[1] The interesting feature of complex **3** is the asymmetry in the Fe^{II}−S bond lengths (2.327(2) and 2.305(2) Å), which shows a difference of 0.022 Å. In complexes **2** and **3**, the two carbonyl groups are disposed in a cis arrangement and are trans to the

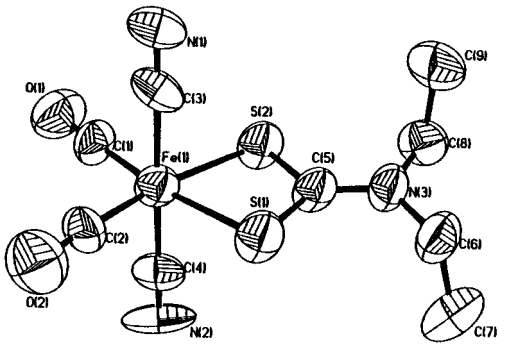

Figure 7. ORTEP drawing and labeling scheme of $[(CN)_2(CO)_2Fe(S,S-C-N(Et)_2)]^-$ with thermal ellipsoid drawn at 50% probability.

Table 4. Selected Bond Distances (Å) and Angles (deg) for Complexes **3**, **6**, and **7**

	Complex **3**		
Fe(1)−C(2)	1.785(6)	Fe(1)−C(1)	1.811(6)
Fe(1)−C(3)	1.897(6)	Fe(1)−C(4)	1.915(6)
Fe(1)−S(1)	2.305(2)	Fe(1)−S(2)	2.327(2)
N(1)−C(3)	1.130(5)	N(2)−C(4)	1.096(6)
N(3)−C(5)	1.316(5)	N(3)−C(6)	1.455(6)
N(3)−C(8)	1.474(6)	S(2)−C(5)	1.709(5)
S(1)−C(5)	1.719(5)		
C(2)−Fe(1)−C(1)	96.8(3)	C(2)−Fe(1)−C(3)	91.9(3)
C(1)−Fe(1)−C(3)	87.3(3)	C(2)−Fe(1)−C(4)	90.9(3)
C(3)−Fe(1)−C(4)	177.1(2)	S(1)−Fe(1)−S(2)	75.02(6)
C(2)−Fe(1)−S(2)	166.7(2)	C(1)−Fe(1)−S(2)	96.4(2)
	Complex **6**		
Fe(1)−C(1)	1.751(5)	Fe(1)−C(2)	1.731(6)
Fe(1)−C(3)	1.899(5)	Fe(1)−O(3)	1.97(2)
Fe(1)−S(1)	2.202(10)	Fe(1)−C(4)	1.939(2)
N(1)−C(3)	1.153(5)	N(2)−C(4)	1.130(4)
C(1)−O(1)	1.140(5)	C(2)−O(2)	1.160(5)
N(3)−O(3)	1.47(2)		
C(1)−Fe(1)−C(2)	92.8(3)	C(1)−Fe(1)−C(3)	92.3(3)
C(2)−Fe(1)−C(3)	87.3(3)	C(1)−Fe(1)−O(3)	172.7(6)
C(2)−Fe(1)−O(3)	93.9(6)	C(3)−Fe(1)−C(4)	177.59(18)
O(3)−Fe(1)−S(1)	89.2(6)		
	Complex **7**		
Fe−C(3)	1.769(4)	Fe−C(4)	1.821(4)
Fe−C(1)	1.892(4)	Fe−C(2)	1.928(3)
Fe−N(3)	1.971(3)	Fe−S(1)	2.3546(9)
S(1)−C(5)	1.723(4)	C(1)−N(1)	1.146(4)
C(2)−N(2)	1.156(4)	C(3)−O(1)	1.145(4)
C(1)−Fe−C(2)	179.67(14)	N(3)−Fe−S(1)	70.71(8)
C(3)−Fe−C(4)	94.62(16)	C(3)−Fe−N(3)	167.86(13)
C(3)−Fe−S(1)	97.52(11)	C(4)−Fe−S(1)	167.64(13)

sulfur atoms. The four-membered FeS_2C rings for complexes **2** and **3** are almost planar with a dihedral angle between FeS_2 and S_2C planes of 5.7° and 0.2°, respectively.

Structures of Complexes 6 and 7. Definitive assignment of the structure of complex **6** was obtained by X-ray crystallography; the structure of *trans*,*cis*-$[(CN)_2(CO)_2Fe(S,O-C_5H_4N)]^-$ unit as PPN^+ salt is shown in Figure 8. The coordination about Fe in $[(CN)_2(CO)_2Fe(S,O-C_5H_4N)]^-$ can be considered as essentially octahedral, with the bite angle of the chelating $[S,O-C_5H_4N]^-$ ligand being 89.2(6)° and the positions trans to the $[S,O-C_5H_4N]^-$ bidentate ligand occupied by two CO ligands. This feature, as observed in complexes **2** and **3**, can be attributed to the electronic influence of the bidentate $[S,O-C_5H_4N]^-$ ligand. Because of disorder of S(1) and O(3), the exact Fe(1)−S(1) and Fe(1)−O(3) bond lengths are poorly determined. The Fe(II)−S bond of length 2.202(10) Å is significantly shorter than the Fe(II)−S distance in complex

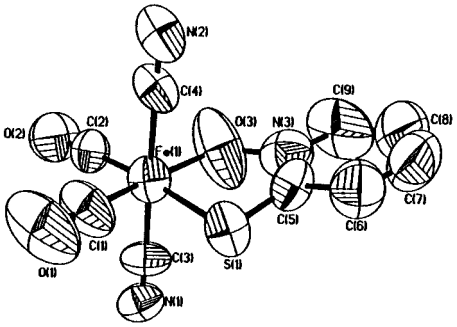

Figure 8. ORTEP drawing and labeling scheme of $[(CN)_2(CO)_2Fe(S,O-C_5H_4N)]^-$ with thermal ellipsoid drawn at 50% probability.

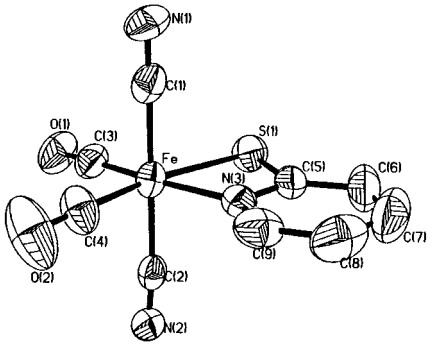

Figure 9. ORTEP drawing and labeling scheme of $[(CN)_2(CO)_2Fe(S,N-C_5H_4)]^-$ with thermal ellipsoid drawn at 50% probability.

7 (2.347(2) Å). The Fe(II)−O bond distance in complex **6** is 1.97(2) Å (Table 4).

The X-ray crystal structure of complex **7** is shown in Figure 9. The bond angles at the Fe^{II} center is considerably distorted from the idealized octahedral limits due to the presence of the four-membered N,S-chelate ring, a characteristic apparent in the internal chelate angle, S(1)−Fe−N(3) of 70.71(8)° (Table 4).[19a] The Fe−S(1) and Fe−N(3) bond lengths, 2.3546(9) and 1.971(3) Å in complex **7**, are comparable to the values of 2.3323(9) and 2.000(3) Å in $[(CN)(CO)Fe(S,N-C_4H_3N)_2]^-$.[13]

Conclusion and Comments

The following are the principal results of this investigation.

1. The iron(II) thiolate cyanocarbonyl complexes **2**, **3**, **6**, and **7** are prepared, respectively, by the reaction of [Na][S−C(S)−R]/[Na][S,O−C_5H_4N]/[Na][S,N−C_5H_4] with $[(CN)_2(CO)_3Fe(Br)]^-$ which was obtained from oxidative addition of BrCN to $[Fe(CO)_4(CN)]^-$.

2. Isotopic shift experiments demonstrate the lability of carbonyl ligands of complexes **2**, **3**, **4**, **5**, **7**, and **8**.

3. Photolysis of THF solutions of complexes **2**, **3**, and **7** at room temperature led to the formation of coordinatively unsaturated iron(II) dicyanocarbonyl thiolate complexes **4**, **5**, and **8**, respectively, with two cyanides occupying cis positions and a vacant site preference trans to the CO ligand.[1−8,27−31] Additionally, density functional theory (DFT) calculations also suggest the architecture of five-coordinate complexes **4**, **5**, and **8** with a vacant site trans to the CO ligand and two CN^- ligands occupying cis positions serves as a conformational preference.[29−31]

4. The strong σ-donor, weak π-acceptor CN^- ligands play a major role in creating and stabilizing a five-coordinate iron(II) center with a vacant coordination site.[13,25]

5. The reversibility of CO ligand binding demonstrates that complexes **2**/**4**, **3**/**5**, and **7**/**8** are photochemically interconvertible. This result may imply the involvement of iron site in the mechanism of hydrogen activation, and can be useful in exploring the key step in H_2 uptake mechanism in [NiFe] hydrogenases.

6. Complexes **4**, **5**, and **8** on binding of the substrate (CO) undergo considerable conformational changes, i.e., *cis,trans*-$[(CN)_2(CO)_2Fe(S,S-C-R)]^-$ converted into *trans,cis*-$[(CN)_2(CO)_2Fe(S,S-C-R)]^-$.

7. The vibrational spectra of the $[Fe^{II}(CN)_2(CO)]$ and $[Fe^{II}(CN)_2(CO)_2]$ units (ν_{CO} and ν_{CN}) found for complexes **4**, **5** and **2**, **3** may be regarded as spectroscopic references for a variety of [NiFe] hydrogenase enzymatic states,[26] and may be the exogenously added CO inhibited state, respectively.[4]

8. The two thiolate ligands $[S,S-COEt]^-$ and $[S,S-C-N(Et)_2]^-$, rendering the $[(CN)_2(CO)Fe]$ unit in different electronic environments, induce different stability to CO ligand.[1-8]

9. All attempts to bind H^- ligand terminally to $[(CN)_2(CO)Fe(S,S-C-R)]^-$ unit were not observed spectroscopically.[29]

This investigation would perhaps allow a more extensive discussion of the inhibition of the hydrogenases by exogenous CO molecule and the photochemical properties of the CO inhibitor complexes.

Experimental Section

Manipulations, reactions, and transfers of samples were conducted under nitrogen according to standard Schlenk techniques or in a glovebox (argon gas). Solvents were distilled under nitrogen from appropriate drying agents (diethyl ether from CaH_2; acetonitrile from CaH_2–P_2O_5; methylene chloride from P_2O_5; hexane and tetrahydrofuran (THF) from sodium benzophenone) and stored in dried, N_2-filled flasks over 4 Å molecular sieves. Nitrogen was purged through these solvents before use. Solvent was transferred to the reaction vessel via stainless steel cannula under positive pressure of N_2. The reagents iron pentacarbonyl, hexamethyldisilazane sodium salt, cyanogen bromide, bis(triphenylphosphoranylidene)ammonium chloride, 2-mercaptopyridine, 2-mercaptopyridine *N*-oxide sodium salt hydrate (Lancaster/Aldrich), sodium xanthogenate (TCI), and diethyldithiocarbamic acid sodium salt (Arcos) were used as received. Compound $[PPN][Fe(CO)_4(CN)]$ was synthesized and characterized by published procedures.[17] Infrared spectra of the carbonyl ν(CO) and cyanide ν(CN) stretching frequencies were recorded on a Bio-Rad Model FTS-185 spectrophotometer with sealed solution cells (0.1 mm) and KBr windows. ^{1}H and ^{13}C NMR spectra were obtained on a Bruker Model AC 200 spectrometer. UV/vis spectra were recorded on a Hewlett-Packard 71 spectrophotometer. Photolysis reactions were carried out in a 100 mL water-cooled Pyrex reactor equipped with a mercury arc 450-W UV lamp inside the reactor. Analyses of carbon, hydrogen, and nitrogen were obtained with a CHN analyzer (Heraeus).

Preparation of $[PPN][(CN)_2(CO)_3Fe(Br)]$ (1). The compounds $[PPN][Fe(CO)_4(CN)]$ (0.5 mmol, 0.365 g) and cyanogen bromide (BrCN) (0.8 mmol, 0.084 g) were dissolved in 8 mL of THF and stirred at ambient temperature for 2 h. The solution was then filtered through Celite and hexane (15 mL) was added to precipitate the orange solid $[PPN][(CN)_2(CO)_3Fe(Br)]$ (0.277 g, 68%). Diffusion of hexane into a THF solution of complex **1** at −15 °C for 4 weeks led to orange crystals suitable for X-ray crystallography. IR (THF): 2139 vw, 2127 vw (ν_{CN}), 2099 m, 2056 s, 2035 m (ν_{CO}) cm^{-1}. Absorption spectrum (THF) [λ_{max}, nm (ϵ, M^{-1} cm^{-1})]: 325(1990) (sh), 383(658). Anal. Calcd for $C_{41}H_{30}BrFeN_3O_3P_2$: C, 60.77; H, 3.73; N, 5.19. Found: C, 60.88; H, 4.03; N, 4.96.

Preparation of *trans,cis*-$[PPN][(CN)_2(CO)_2Fe(S,S-C-R)]$ (R = OEt (2), $N(Et)_2$ (3)). Sodium xanthogenate (0.029 g, 0.2 mmol) (or diethyldithiocarbamic acid sodium salt, 0.045 g, 0.2 mmol) was added to a THF solution containing 0.162 g (0.2 mmol) of complex **1** and stirred at 50 °C for 3h. The reaction mixture was then filtered to separate the precipitate NaBr, and then diethyl ether was added to precipitate the yellow semisolid *trans,cis*-$[PPN][(CN)_2(CO)_2Fe(S,S-C-OEt)]$ (**2**) (0.075 g, 45%) (yellow semisolid *trans,cis*-$[PPN][(CN)_2(CO)_2Fe(S,S-C-N(Et)_2)]$ (**3**),(0.090 g, 52%)). Recrystallization from concentrated THF solution with diethyl ether diffusion gave yellow crystals used in the X-ray diffraction study. Complex **2**: IR: 2122 vw, 2112 w (ν_{CN}), 2038 vs, 1984 vs (ν_{CO}) cm^{-1} (THF); 2125 vw,br, 2112 w,br (ν_{CN}), 2053 vs, 2006 vs (ν_{CO}) cm^{-1} (MeOH). ^{1}H NMR (CD_3CN): δ 1.37 (t), 1.38 (t), 4.55 (q), 4.58 (q) ($O-CH_2-CH_3$) ppm.[32] ^{13}C NMR (CD_3CN): δ 214.04 (s), 209.08 (s) ppm (CO). Absorption spectrum (CH_2Cl_2) [λ_{max}, nm (ϵ, M^{-1} cm^{-1})]: 332(2111), 342(1656) (sh). Anal. Calcd for $C_{43}H_{35}O_3N_3P_2S_2Fe$: C, 62.70; H, 4.28; N, 5.10. Found: C, 62.47; H, 4.43; N, 5.63. Complex **3**: IR: 2119 vw, 2112 w (ν_{CN}), 2027 vs, 1973 vs (ν_{CO}) cm^{-1} (THF); 2120 vw,br, 2108 w,br (ν_{CN}), 2043 vs, 1996 vs (ν_{CO}) cm^{-1} (MeOH). ^{1}H NMR (CD_3CN): δ 1.17 (t), 1.20 (t), 3.64 (q), 3.67 (q) ppm ($N-CH_2-CH_3$).[32] ^{13}C NMR (CD_3CN): δ 214.1 (s), 209.6 (s) ppm (CO). Absorption spectrum (CH_2Cl_2) [λ_{max}, nm (ϵ, M^{-1} cm^{-1})]: 332(2111), 342(1656) (sh). Anal. Calcd for $C_{45}H_{40}N_4O_2S_2FeP_2$: C, 63.53; H, 4.74; N, 6.59. Found: C, 63.64; H, 4.88; N, 6.97.

Preparation of *trans,cis*-$[PPN][(CN)_2(CO)_2Fe(S,O-C_5H_4N)]$ (6). A solution containing 0.324 g (0.4 mmol) of complex **1** and 0.06 g (0.4 mmol) of $[Na][S,O-C_5H_4N]$ in THF (8 mL) was stirred at ambient temperature overnight. The resulting mixture was filtered to remove [Na][Br] and then diethyl ether (15 mL) was added to precipitate the dark purple solid *trans,cis*-$[PPN][(CN)_2(CO)_2Fe(S,O-C_5H_4N)]$ (0.063 g, 19%). Recrystallization from saturated THF solution with diethyl ether diffusion at −15 °C gave dark purple crystals suitable for X-ray crystallography. The THF solution of complex **6** was thermally unstable which on stirring at 40 °C overnight was completely converted to complex **7** as revealed from the IR spectrum. IR (THF): 2121 vw, 2109 w (ν_{CN}), 2041 vs, 1982 vs (ν_{CO}) cm^{-1}. ^{1}H NMR (CD_3CN): δ 7.85 (d), 7.01 (t), 6.72 (d) ($S,O-C_5H_4N$) ppm. Absorption spectrum (CH_3CN) [λ_{max}, nm (ϵ, M^{-1} cm^{-1})]: 352(2035), 487(404) (sh). Anal. Calcd for $C_{45}H_{34}O_3SN_4FeP_2$: C, 65.23; H, 4.14; N, 6.76. Found: C, 64.83; H, 4.35; N, 6.54.

Preparation of *trans,cis*-$[PPN][(CN)_2(CO)_2Fe(S,N-C_5H_4)]$ (7). Complex **1** (0.4 mmol, 0.324 g) and $[Na][S,N-C_5H_4]$ (0.4 mmol, 0.053 g) were dissolved in 8 mL of THF and stirred overnight under nitrogen at ambient temperature. The resulting mixture was then filtered through Celite to remove [Na][Br] and diethyl ether (15 mL) was added to precipitate the light yellow solid *trans,cis*-$[PPN][(CN)_2(CO)_2Fe(S,N-C_5H_4)]$ (0.104 g, 32%). Diffusion of diethyl ether into THF solution of complex **7** at −15 °C for 4 weeks led to yellow crystals suitable for X-ray crystallography. IR (THF): 2124 vw, 2113 w (ν_{CN}), 2036 vs, 1983 vs (ν_{CO}) cm^{-1}. ^{1}H NMR (C_4D_8O): δ 8.11 (d), 7.25 (t), 6.63 (t), 6.52 (d) ($S,N-C_5H_4$) ppm. ^{13}C NMR (CD_3CN): δ 214.4 (d), 210.0 (d) ppm (CO) ($J^{13}C,^{13}C$ = 9 Hz). Absorption spectrum (THF) [λ_{max}, nm (ϵ, M^{-1} cm^{-1})]: 347(3498), 422(465) (sh). Anal. Calcd for $C_{45}H_{34}O_2SN_4FeP_2$: C, 66.51; H, 4.22; N, 6.89. Found: C, 66.36; H, 4.23; N, 6.71.

Photolysis of THF Solution of Complexes 2, 3, and 7. Complex **2** (0.2 mmol, 0.165 g) (**3**: 0.2 mmol, 0.171 g; **7**: 0.2 mmol, 0.163 g) was dissolved in 10 mL of THF and irradiated by UV lamp under CO atmosphere at 20 °C for 15 min. The solution was then monitored with FTIR. The IR spectra 2113 w, 2105 w (ν_{CN}), 1996 vs (ν_{CO}) (THF) cm^{-1} indicated the formation of $[PPN][(CN)_2(CO)Fe(S,S-C-OEt)]$ (**4**) (2109 w, 2102 w (ν_{CN}), 1985 vs (ν_{CO}) (THF) cm^{-1} and 2111 w, 2103 w (ν_{CN}), 1996 vs (ν_{CO}) (THF) cm^{-1} showed the formation of $[PPN][(CN)_2(CO)Fe(S,S-C-N(Et)_2)]$ (**5**) and $[PPN][(CN)_2(CO)Fe(S,N-C_5H_4)]$ (**8**) individually). The THF solutions of complexes **4**, **5**,

(32) Edgar, B. L.; Duffy, D. J.; Palazzotto, M. C.; Pignolet, L. H. *J. Am. Chem. Soc.* **1973**, *95*, 1125.

Table 5. Crystallographic Data of Complexes **1**·THF and **2**

	1·THF	**2**
chem formula	$C_{45}H_{38}N_3O_4BrFeP_2$	$C_{43}H_{35}N_3O_3S_2FeP_2$
fw	882.48	823.65
cryst syst	monoclinic	monoclinic
space group	$P2_1/c$	$P2_1/c$
λ, Å (Mo Kα)	0.7107	0.7107
a, Å	12.2022(2)	12.157(3)
b, Å	13.2023(2)	13.341(3)
c, Å	25.5672(2)	25.364(6)
α, deg	90	90
β, deg	90.834(1)	92.462(5)
γ, deg	90	90
V, Å^3	4118.37(10)	4109.8(17)
Z	4	4
d_{calcd}, g cm^{-3}	1.423	1.331
μ, mm^{-1}	1.461	0.589
T, K	150(1)	295(2)
R	0.0841[a]	0.0680[a]
R_{WF}^2	0.2691[b]	0.1337[b]
GOF	1.119	1.047

[a] $R = \sum|(F_o - F_c)|/\sum F_o$. [b] $R_{WF}^2 = \{\sum w(F_o^2 - F_c^2)^2/\sum[w(F_o^2)^2]\}^{1/2}$.

Table 6. Crystallographic Data of Complexes **3**, **6**, and **7**

	3	**6**	**7**
chem formula	$C_{45}H_{40}N_4O_2S_2FeP_2$	$C_{45}H_{34}O_3SN_4FeP_2$	$C_{45}H_{34}O_2SN_4FeP_2$
fw	850.72	828.61	812.61
cryst syst	monoclinic	monoclinic	monoclinic
space group	$P2_1/n$	$P2_1/n$	$P2_1/n$
λ, Å (Mo Kα)	0.7107	0.7107	0.7107
a, Å	16.982(2)	17.061(1)	17.6478(2)
b, Å	15.9068(19)	15.871(1)	13.1862(2)
c, Å	17.576(2)	17.345(2)	17.8391(3)
α, deg	90	90	90
β, deg	115.476(3)	117.404(2)	104.9324(7)
γ, deg	90	90	90
V, Å^3	4286.1(9)	4169.7(6)	4011.10(10)
Z	4	4	4
d_{calcd}, g cm^{-3}	1.318	1.320	1.346
μ, mm^{-1}	0.566	0.533	0.551
T, K	293(2)	295(2)	150(1)
R	0.0473[a]	0.0573[a]	0.0525[a]
R_{WF}^2	0.0702[b]	0.0751[b]	0.0919[b]
GOF	0.604	0.898	1.036

[a] $R = \sum|(F_o - F_c)|/\sum F_o$. [b] $R_{WF}^2 = \{\sum w(F_o^2 - F_c^2)^2/\sum[w(F_o^2)^2]\}^{1/2}$.

and **8** are stable at low temperature ($T < 0$ °C). The THF solutions of complexes **5** and **8** were stirred at ambient temperature (25 °C) overnight; the IR spectra revealed the formation of complexes **3** and **7** along with the insoluble solids, presumably [PPN][S,S−C−N(Et)$_2$] and [PPN][S,N−C$_5$H$_4$], respectively. THF solutions of complexes **4**, **5**, and **8** were reduced to 3 mL and hexane (10 mL) was then added to precipitate the orange semisolid complexes **4**, **5**, and **8**. The thermally unstable products **4**, **5**, and **8** were isolated, individually, by removing the solvent (since decomposition occurred under vacuum, the yields of the semisolid complexes were difficult to determine). Complex **4**: IR (THF): 2113 w, 2105 w (ν_{CN}), 1996 vs (ν_{CO}) cm^{-1}. ^{1}H NMR (CD$_3$CN): δ 4.49 (q), 1.34 (t) (O−CH$_2$CH$_3$) ppm. ^{13}C NMR (CD$_3$CN): δ 210.79 (s) ppm (CO). Absorption spectrum (THF) [λ_{max}, nm (ϵ, M^{-1} cm^{-1})]: 336(1082), 360(908). Complex **5**: IR (THF): 2109 w, 2102 w (ν_{CN}), 1985 vs (ν_{CO}) cm^{-1}. ^{1}H NMR (CD$_3$CN): δ 1.16 (t), 1.20 (t), 3.61 (q), 3.64 (q) (N−CH$_2$CH$_3$) ppm. ^{13}C NMR (CD$_3$CN): δ 212.5 (s) ppm (CO). Absorption spectrum (THF) [λ_{max}, nm (ϵ, M^{-1} cm^{-1})]: 383(2395), 506(736), 593(575). Complex **8**: IR (THF): 2111 w, 2103 w (ν_{CN}), 1996 vs (ν_{CO}) cm^{-1}. ^{1}H NMR (C$_4$D$_8$O): δ 7.77 (d), 7.21 (t), 6.60 (t), 6.44 (d) (S,N−C$_5$H$_4$) ppm. ^{13}C NMR (CD$_3$CN): δ 212.7 (s) ppm (CO). Absorption spectrum (THF) [λ_{max}, nm (ϵ, M^{-1} cm^{-1})]: 334(5218), 408(3296).

Crystallography. Crystallographic data of complexes **1**, **2**, **3**, **6**, and **7** are summarized in Tables 5 and 6 and in the Supporting Information. The crystals of **1**, **2**, **3**, **6**, and **7** are chunky. The crystals of **1**, **2**, **3**, **6**, and **7** chosen for X-ray diffraction studies measured 0.33 × 0.12 × 0.10 mm, 0.08 × 0.08 × 0.4 mm, 0.08 × 0.17 × 0.34 mm, 0.211 × 0.211 × 0.42 mm, and 0.2 × 0.18 × 0.15 mm, respectively. Each crystal was mounted on a glass fiber. Diffraction measurements for complexes **2**, **3**, **6**, and **7** were carried out at 295(2) K (150(1) K for complexes **1** and **7**) on a Siemens SMART CCD diffractometer with graphite-monochromated Mo Kα radiation (λ 0.7107 Å) and θ between 1.67° and 27.50° for complex **1**, between 1.61° and 25.00° for complex **2**, between 1.39° and 27.58° for complex **3**, between 1.39° and 27.54° for complex **6**, and between 2.36° and 27.50° for complex **7**. Least-squares refinement of the positional and anisotropic thermal parameters for the contribution of all non-hydrogen atoms and fixed hydrogen atoms was based on F^2. A SADABS[33] absorption correction was made. The SHELXTL[34] structure refinement program was employed. In the case of complex **2**, the OCH$_2$CH$_3$ group (shown in Figure 6) is found at disordered positions (O(3)C(6)C(7):O(3)′C(6)′C(7)′ = 2/3:1/3) and were refined by partial occupancies; in the case of **6** one sulfur and one oxygen atom (S(1) and O(3) as shown in Figure 8) are found at disordered positions and were refined by partial occupancies.

Acknowledgment. We thank the National Science Council (Taiwan) for support of this work. We also thank Prof. Marcetta Y. Darensbourg for helpful suggestions.

Supporting Information Available: X-ray crystallographic file in CIF format for the structure determinations of [PPN][(CN)$_2$(CO)$_3$Fe(Br)], [PPN][(CN)$_2$(CO)$_2$Fe(S,S−C−OEt)], [PPN][(CN)$_2$(CO)$_2$Fe(S,S−C−N(Et)$_2$)], [PPN][(CN)$_2$(CO)$_2$Fe(S, O−C$_5$H$_4$N)], and [PPN][(CN)$_2$(CO)$_2$Fe(S,N−C$_5$H$_4$)]. Tables of crystal data and structure refinement, atomic coordinates and displacement parameters, and bond lengths and angles (PDF). This material is available free of charge via the Internet at http://pubs.acs.org.

JA011504F

(33) Sheldrick, G. M. *SADABS, Siemens Area Detector Absorption Correction Program*; University of Göttingen: Göttingen, Germany, 1996.
(34) Sheldrick, G. M. *SHELXTL, Program for Crystal Structure Determination;* Siemens Analytical X-ray Instruments Inc.: Madison, WI, 1994.